frontiers | Frontiers in Energy Research

TYPE Original Research
PUBLISHED 15 September 2022
DOI 10.3389/fenrg.2022.993376

OPEN ACCESS

EDITED BY
Paola Brachi,
National Research Council (CNR), Italy

REVIEWED BY
Xinying Liu,
University of South Africa, South Africa
Fehmi Akgun,
TUBITAK Marmara Research Centre Energy Institute, Turkey

*CORRESPONDENCE
Umesh Pandey,
umesh.pandey@ntnu.no

SPECIALTY SECTION
This article was submitted to Bioenergy and Biofuels, a section of the journal Frontiers in Energy Research

RECEIVED 13 July 2022
ACCEPTED 19 August 2022
PUBLISHED 15 September 2022

CITATION
Pandey U, Putta KR, Rout KR, Rytter E, Blekkan EA and Hillestad M (2022), Conceptual design and techno-economic analysis of biomass to liquid processes.
Front. Energy Res. 10:993376.
doi: 10.3389/fenrg.2022.993376

Conceptual design and techno-economic analysis of biomass to liquid processes

Umesh Pandey*, Koteswara R. Putta, Kumar R. Rout, Erling Rytter, Edd A. Blekkan and Magne Hillestad

Norwegian University of Science and Technology, Trondheim, Norway

Advanced biofuels are produced by upgrading the syncrude from biomass gasification and subsequent Fischer-Tropsch (FT) synthesis. The technology is termed biomass to liquid process (BtL) and can be categorized into conventional BtL and novel BtL processes. The conventional BtL utilizes a water gas shift reaction, while novel BtL utilizes an external energy source to meet H_2 demand in FT synthesis. Six different process routes, two based on the conventional BtL and four based on novel BtL with solid oxide electrolyzer cell (SOEC) integration, are developed and evaluated based on the process performance and economic viability. The results show that the novel BtL technology can retain up to 96% of carbon in the biomass (up from 46% in the conventional BtL process), and syncrude production is increased by a factor of 2.4 compared to the conventional BtL process. The economic analysis shows that SOEC costs and electricity prices are critical for the viability of the novel BtL plants. For current electrical power and SOEC cost, optimizing the conventional BtL process offers the best process route for producing advanced biofuels (minimum selling price of syncrude (MSP): $1.73/L). Further improvement in SOEC technology could see a dramatic drop in SOEC costs. With a reduced SOEC installation cost of $230/kW, directly adding SOEC-H_2 in FT synthesis and recycling excess CO_2 offers the best route for syncrude production. For this SOEC cost, the MSP is estimated to be $1.38/L, 20% lower than the MSP for the optimized conventional BtL process.

KEYWORDS

BTL process, syncrude production, techno-economic analysis, Fischer-Tropsch synthesis, advanced biofuel

1 Introduction

Addressing the climate crisis due to fossil fuel-related CO_2 emissions requires comprehensive action by diversifying energy sources in all sectors. The EU and Norwegian Environment Agency have envisioned diversifying the energy mix in the transportation sectors by deploying electric vehicles, advanced biofuels, and other low-carbon fuels (European Commission, 2020). The Norwegian environment agency has mandated 4% of the road transportation and 0.5% of the aviation industry demand to be met by utilizing advanced biofuels since 2020 (Miljødirektoratet, 2022). Advanced biofuel

production incorporates biomass gasification and subsequent catalytic conversion to liquid biofuels *via* Fischer-Tropsch synthesis (Swanson et al., 2010; Dimitriou et al., 2018; Hillestad et al., 2018; Kreutz et al., 2020). The product from the FT synthesis is rich in linear paraffin, which can be upgraded to produce advanced biofuel. The advanced biofuel has similar physical and chemical characteristics to diesel/jet fuel. The fuel can be blended into aviation fuels to meet the EU directive and Norwegian Environment Agency mandates. The plant incorporating these process concepts are called biomass to liquid (BtL) plants. Similar technology of diesel/jet fuel production *via* gasification and FT synthesis is employed on a commercial scale in Sasol plants in South Africa (Spath and Dayton, 2003) and Shenhua Ningmei plants in China (Larson et al., 2012) (coal to liquid), and in Bintulu Shell MDS in Malaysia and Shell's Peral GtL in Qatar (natural gas to liquid) (Carlsson, 2005).

The BtL plants are relatively newer, and few pilot-scale and small-scale BtL plants have been built in recent years (Kolb et al., 2013; Hofbauer et al., 2019). Several studies have tried to bridge the knowledge gap by investigating the techno-economic aspect of the commercial-scale BtL plant (Swanson et al., 2010; Villanueva Perales et al., 2011; Banerjee, 2012; Bernical et al., 2013; Albrecht et al., 2017; Dietrich et al., 2018; Dimitriou et al., 2018; Hillestad et al., 2018; Neuling and Kaltschmitt, 2018; Michailos and Bridgwater, 2019; Kreutz et al., 2020). The BtL process employs five essential steps to produce biofuels from biomass: pre-treatment, gasification, syngas clean-up and conditioning, fuel synthesis, and product upgrading. The BtL process can be differentiated into two distinct processes: the conventional BtL process (Swanson et al., 2010; Villanueva Perales et al., 2011; Banerjee, 2012; Bernical et al., 2013; Albrecht et al., 2017; Dietrich et al., 2018; Dimitriou et al., 2018; Hillestad et al., 2018; Neuling and Kaltschmitt, 2018; Michailos and Bridgwater, 2019; Kreutz et al., 2020) and the power and BtL or novel BtL process (Bernical et al., 2013; Dietrich et al., 2018; Hillestad et al., 2018; Dieterich et al., 2020). These concepts differ in how the hydrogen demand is met in the FT synthesis. The H_2/CO usage ratio in FT synthesis is ca. 2.05. The H2/CO ratio out of the biomass gasifier is ca 0.6–1.0. It should be increased further (preferably to ca. 2.05) to avoid accelerated deactivation of the FT catalyst and maintain stable production of the FT syncrude (Pandey et al., 2021). The conventional BtL processes with FT synthesis over a cobalt catalyst utilize water-gas shift reactions to raise the H_2/CO ratio to ca. 2.05 (Swanson, 2009; Villanueva Perales et al., 2011; Zhu et al., 2011; Banerjee, 2012; Bernical et al., 2013; Leibbrandt et al., 2013; Holmgren, 2015; Rafati et al., 2017; Dietrich et al., 2018; Dimitriou et al., 2018; Hillestad et al., 2018; Neuling and Kaltschmitt, 2018; Michailos and Bridgwater, 2019; Kreutz et al., 2020). This produces CO_2. The excess CO_2 is removed using an acid gas removal unit. Removing excess CO_2 reduces the carbon efficiency of the conventional BtL processes. The prior studies with conventional BtL processes reported carbon efficiency of 16%–38% for a conventional BtL plant (Swanson, 2009; Villanueva Perales et al., 2011; Banerjee, 2012; Albrecht et al., 2017; Dimitriou et al., 2018; Hillestad et al., 2018; Neuling and Kaltschmitt, 2018; Michailos and Bridgwater, 2019; Kreutz et al., 2020). For the novel BtL processes, the hydrogen demand is either met solely through external sources (Hillestad et al., 2018; Dieterich et al., 2020) or a combination of external sources and the water gas shift reaction (Bernical et al., 2013). The prior techno-economic study on novel BtL process incorporated renewable energy powered water electrolysis (Dietrich et al., 2018) or high-temperature steam electrolysis (Bernical et al., 2013; Hillestad et al., 2018) to meet the hydrogen demand in the FT synthesis. Hillestad et al. (2018) proposed the integration of solid oxide electrolyzer cells (SOEC) to produce H_2, which is then utilized to achieve a reverse water gas shift reaction (RWGS) and increase the H_2/CO ratio to the desired level. The RWGS reaction converts CO_2 to CO and thus decreases the loss of carbon as CO_2. This improves the carbon efficiency of the process to more than 90% and increases the total syncrude production from the limited biomass resources. Hillestad et al. (2018) highlighted that the novel BtL technology offers better economic viability than the conventional BtL plants. However, the economic performance is highly susceptible to volatile electricity prices and future prices of the SOEC units.

This study assesses six different BtL process concepts for small-scale BtL plants to produce syncrude from forest residues (wood chips). Two cases (Case I and Case II) are based on conventional process concepts, and the other four cases (Case III-IV) are novel process concepts that improve on the process integration of SOEC to BtL processes proposed by Hillestad et al. (2018). The proposed improvements consider different process alternatives related to SOEC integration and excess CO_2 handling. In addition, the process recommendation of the optimization study by Pandey et al. (2022) is utilized to optimize the syncrude production in the FT synthesis. The current study aims to outline potential routes for biofuel production utilizing two process concepts (six different process routes in total) and estimate the economic viability for variability in the electricity prices and SOEC costs. Norwegian forest owners' association estimates the total forest residues from Norwegian forests to be 11.4 Mm^3 (ca. 2000 wtph) (Norges Skogeierforbund, 2018). This study considers a small-scale BtL plant with a biomass feed of 15.9 wtph to produce the advanced biofuel. The small-scale BtL plant aims to fulfill the advanced biofuel demand in the Norwegian markets. This study does not consider upgrading the syncrude to jet/diesel fuel. The syncrude upgrading could be performed in the existing crude oil upgrading infrastructure and mixed with the aviation and road transportation fuels to achieve 0.5% and 4% of the total demand, respectively.

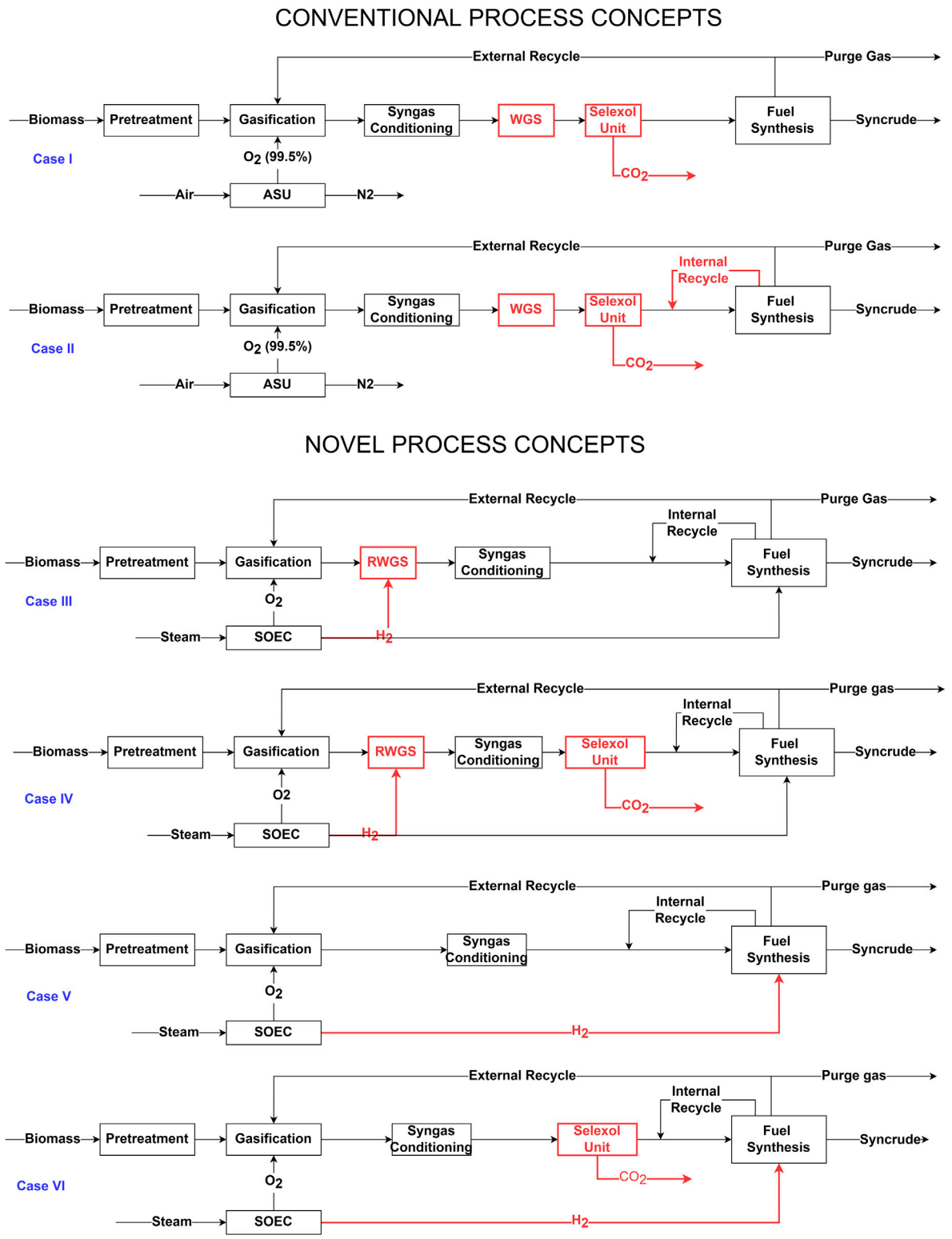

FIGURE 1
Simplified block diagram for different process concepts. Case I: Conventional BtL process with WGS and Selexol process and once-through FT synthesis. The H_2/CO ratio of the feed in FT synthesis is 2.05. Case II: Case I with the introduction of internal recycling in FT synthesis. The H_2/CO ratio of the feed in FT synthesis is optimized to 1.69. Case III: Integration of RWGS to the novel BtL process. Case IV: Case III with the removal of excess CO_2 in the selexol unit. Case V: Direct utilization of H_2 from SOEC in fuel synthesis. Case VI: Case V with the removal of excess CO_2 in the Selexol unit.

2 The process concepts

2.1 Conventional biomass to liquid process

Techno-economic studies of conventional BtL process considered biomass gasification and subsequent catalytic conversion using Fischer-Tropsch (FT) synthesis to produce advanced biofuels (Swanson, 2009; Villanueva Perales et al., 2011; Zhu et al., 2011; Banerjee, 2012; Leibbrandt et al., 2013; Holmgren, 2015; Rafati et al., 2017; Dimitriou et al., 2018; Hillestad et al., 2018; Neuling and Kaltschmitt, 2018; Michailos and Bridgwater, 2019; Kreutz et al., 2020). In biomass gasification using oxygen as a gasifying agent, the H_2/CO ratio is usually between 0.6 and 1.0 (Ravaghi-Ardebili et al., 2014). The FT synthesis over a cobalt catalyst requires H_2/CO ratio above 1 throughout the reactor to avoid catalyst degradation (Storsæter et al., 2005; Dalai and Davis, 2008; Swanson, 2009; Gavrilović et al., 2018). The FT synthesis's H2/CO usage ratio over a cobalt catalyst is ca. 2.05 and varies with the temperature and gas partial pressures (Pandey et al., 2021). The conventional BtL process concepts utilize a water gas shift reaction (WGS) to increase the H_2/CO ratio from 0.6 to 1.0 to ca 2.05 (Swanson, 2009; Villanueva Perales et al., 2011; Zhu et al., 2011; Banerjee, 2012; Leibbrandt et al., 2013; Holmgren, 2015; Rafati et al., 2017; Dimitriou et al., 2018; Hillestad et al., 2018; Neuling and Kaltschmitt, 2018; Michailos and Bridgwater, 2019; Kreutz et al., 2020). The water-gas shift reaction is shown in Eq. 1.

$$CO + H_2O \rightarrow CO_2 + H_2 \quad \Delta H = -41\,\mathrm{kJ/mol} \tag{1}$$

The net effect of the WGS is the conversion of CO to H_2 and CO_2, which will maintain the H_2/CO ratio of the syngas to ca. 2.05. At the same time, a lot of CO_{2s} is produced. The conversion increases overall CO_2 concentration downstream and requires a CO_2 removal process to avoid the accumulation of excess CO_2 in the system. The conventional BtL processes utilize an acid gas removal unit to remove excess CO_2 in the system. In this study, two process concepts utilizing the aforementioned process steps are considered in the techno-economic analysis and compared with novel BtL process concepts.

2.1.1 Case I

Figure 1 shows a block flow diagram and highlights key differences between different BtL process concepts considered in the present study. Case I in Figure 1 is similar to a conventional BtL process described by Michailos and Bridgwater (Michailos and Bridgwater, 2019) and prior techno-economic studies (Swanson, 2009; Villanueva Perales et al., 2011; Banerjee, 2012; Dimitriou et al., 2018; Hillestad et al., 2018; Neuling and Kaltschmitt, 2018; Michailos and Bridgwater, 2019; Kreutz et al., 2020). The process incorporates gasification, water gas shift, CO_2 removal unit, and fuel synthesis as primary processes. The fuel synthesis utilizes single-stage FT synthesis where the per pass CO conversion in FT reactors is set to 40%, and the H_2/CO ratio of the reactor feed is maintained at 2.05. In contrast to the other study (Michailos and Bridgwater, 2019), this study employs fixed bed FT reactors in fuel synthesis. The FT reactor coolant temperature is maintained at 210.6°C, and the syngas feed is heated to 200°C before being fed to the FT reactors. In contrast to other studies (Swanson, 2009; Villanueva Perales et al., 2011; Banerjee, 2012; Dimitriou et al., 2018; Hillestad et al., 2018; Neuling and Kaltschmitt, 2018; Michailos and Bridgwater, 2019; Kreutz et al., 2020), the surplus process heat is assumed to be sold to the industrial consumer instead of converted to electrical power. The process also consists of external recycling of tail gas to the gasifier with the external recycle ratio optimized to maintain N_2 concentration at 5 mol% in the syngas. The detailed process flow diagram and stream flow for Case I can be found in supporting information B.1 and B.2. The detailed process flow diagram and stream flows for the pre-treatment process can be found in supporting information A.1 and A.2.

2.1.2 Case II

As shown in Figure 1, Case II is similar to Case I. The key differences lie in the H_2/CO ratio of the feed and per pass CO conversion in FT synthesis and the introduction of internal recycling in the fuel synthesis process. These parameters are modified based on the path optimization results as described in Pandey et al. (2022). The H_2/CO ratio in the FT reactor feed is set to 1.7, and CO conversion per pass in the reactor is set to 60%. The internal recycle ratio is optimized, so the N_2 mole fraction in the reactor feed stream is less than 10 mol%. The external recycle ratio is optimized to maintain the N_2 mole fraction in makeup gas to below 5 mol%. The detailed process flow diagram (excluding the pre-treatment process) and stream flows of Case II can be found in supporting information C.1 and C.2.

2.2 Novel biomass to liquid process with solid oxide electrolyzer cell integration

The conventional biomass to liquid process based on gasification and FT synthesis has a carbon efficiency of 18%–38% and energy efficiency of 32%–38% (Swanson, 2009; Villanueva Perales et al., 2011; Banerjee, 2012; Albrecht et al., 2017; Dimitriou et al., 2018; Hillestad et al., 2018; Neuling and Kaltschmitt, 2018; Michailos and Bridgwater, 2019; Kreutz et al., 2020). However, due to the water-gas shift reaction, a lot of carbon ends up as CO_2, leading to a carbon efficiency lower than 50%. This is primarily because of two reasons: 1) lower H/C ratio in the biomass and 2) gasification is endothermic. Due to the endothermic reactions, energy must be added to enhance the conversion of carbon to CO instead of to CO_2. In addition, a lower H/C ratio means that one must either rely on a WGS reaction to make up for the required H_2/CO ratio in the syngas

feed or add external H_2. Hillestad et al. (2018) integrated an electrolyzer as a hydrogen source to increase the carbon efficiency to as high as 90% by feeding H_2 from SOEC to the reverse water gas shift (RWGS) process. The study considered a 3-stage FT synthesis and used a fraction of H_2 from SOEC to achieve desired H_2/CO ratio in the 2nd and 3rd stages. A prior study by Pandey et al. (2022) has shown that operating FT synthesis with internal recycling in two stages with optimal CO conversion of 60% per pass and 96.1% overall CO conversion, optimal H_2/CO ratio of 1.7, and optimal operating temperature of 210.6°C is economically beneficial. This study incorporates the recommendation of optimization study along with SOEC integration. This study considers SOEC integration to achieve higher carbon efficiency and energy efficiency with optimal fuel synthesis. Techno-economic analysis of four different process concepts with SOEC integration, Case III, IV, V, and VI, are performed in this study.

2.2.1 Case III and IV

As shown in Figure 1, Case III and IV correspond to the processes with RWGS integration where high-temperature H_2 from the SOEC is mixed with the effluent gas from the gasifier. It fulfills two objectives in the process. First, a fraction of CO_2 is converted to CO, thus reducing the carbon loss and thereby improving the overall carbon efficiency of the process. In addition, the unconverted H_2 is used to maintain the desirable H_2/CO ratio in the first stage of the FT synthesis. A fraction of H_2 from SOEC is fed to the second stage of FT synthesis to replenish the H_2/CO ratio in the unconverted syngas after the first stage. The detailed process flow diagram (excluding the pre-treatment process) and stream flow for Case III can be found in supporting information D.1–D.2.

In contrast to Case III, a selexol unit is also incorporated in Case IV to remove unconverted CO_2 in the gas out of the RWGS process. As with the conventional process, CO_2 removal efficiency in the selexol unit is taken as 90%. Removing excess CO_2 in the selexol unit in Case IV lowers the carbon efficiency compared to Case III, but it reduces the overall electrical load in the SOEC. The idea here is to understand the techno-economic effect of removing excess CO_2 in Case IV and compare it with Case III, where all the excess CO_2 is recycled. The detailed process flow diagram and stream flow for Case IV can be found in supporting information E.1–E.2.

2.2.2 Case V and VI

As shown in Figure 1, Case V and VI correspond to the process where the H_2 from SOEC is directly added to the syngas feed to achieve a desirable H_2/CO ratio in the FT synthesis. A significant advantage of direct utilization compared to Case III and IV is that additional design modifications for RWGS are unnecessary. The carbon efficiency is expected to be lower than in Case III, but the overall capital investment is much lower than in Case III and Case IV. The excess CO_2 in Case V is still recycled with a small purge. The lack of a dedicated RWGS process means that overall material flow is higher in Case V than in Case III. In Case VI, a selexol unit is incorporated to study the effect of excess CO_2 removal in the process. The detailed process flow diagram and stream flow for Case V and VI can be found in supporting information F.1–F.2 and G.1–G.2, respectively.

3 Process modeling and simulation

3.1 The biomass

Biomass is organic materials originating from trees, plants, agriculture, or biogenic wastes. The Norwegian law defines biofuels as fuel derived from the residues of agriculture, aquaculture, fisheries, and forestry (LOVDATA, 2022). The biomass feed considered in this study is forest residues identical to those used in the previous study by the same author (Putta et al., 2022). The ultimate and proximate analysis of the biomass feed is summarized in supporting information H.4. For the Aspen Plus modeling, biomass is defined as a nonconventional component as Aspen Plus lacks a predefined component with biomass characteristics. The HHV of biomass is estimated in Aspen Plus using Boie correlation (Boie, 1953), and LHV is then calculated from HHV to be 18.9 MJ/kg. The total biomass feed is 15.9 wtph and is kept identical for all the process concepts. The feed flow considered here is suitable for small-scale BtL plants which aim to fulfill the demand in the Norwegian aviation industry.

3.2 Pre-treatment of biomass

The biomass comes in various sizes and moisture content and thus requires preprocessing before being fed to the gasifier. The pre-treatment includes size reduction, drying, and torrefaction (Swanson, 2009; Villanueva Perales et al., 2011; Banerjee, 2012; Haarlemmer et al., 2014; Albrecht et al., 2017; Dimitriou et al., 2018; Hillestad et al., 2018; Neuling and Kaltschmitt, 2018; Michailos and Bridgwater, 2019; Kreutz et al., 2020). The block diagram of the pre-treatment process is shown in Figure 2. The drying process is a very energy-intensive process, and various studies have considered using either hot gas or superheated steam for the drying process (Hillestad et al., 2018; Michailos and Bridgwater, 2019). Drying of biomass reduces the overall high-quality energy requirement in the gasifier. Instead, waste heat can be utilized for the drying process. A rotary dryer is considered in this study, where FT steam is utilized to dry the biomass. The process is modeled in Aspen Plus as a combination of a yield reactor and heat exchanging unit. The yield reactor simulates the removal of water from the biomass and thus reducing the moisture content from 40% to 4.7%. In the heat exchanging unit, the biomass and free water temperature are increased to 110°C at atmospheric pressure.

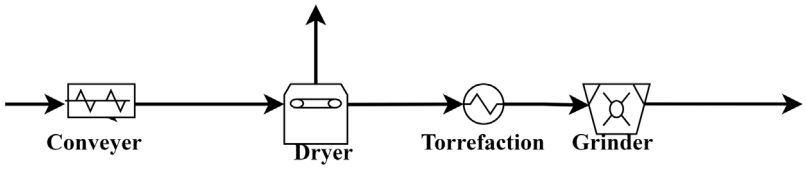

FIGURE 2
Block flow diagram of pre-treatment of biomass.

The dry biomass is torrefied by heating to 250°C and ground before being fed to the entrained flow gasifier. As Tapaswi et al. reported, torrefaction of biomass reduces the energy required for the grinding process. The torrefaction process also releases volatile components, which are fed to the gasifier. As entrained flow gasification in this study requires a smaller particle size (Swanson, 2009; Hillestad et al., 2018), the torrefied biomass is reduced to less than 1 mm in size in a grinder to achieve very high carbon conversion. The grinding energy requirement is 2% of the HHV of biomass, as reported by Hoseinzade and Adams (2019).

3.3 Biomass gasification

Gasification is an exciting process where biomass thermally dissociates into gaseous products. This study considers entrained flow gasification. An entrained flow gasifier (EF-gasifier) is usually operated between 1,100°C and 1,600°C with either external assisted heating or partial oxidation of the biomass feed (Swanson et al., 2010; Villanueva Perales et al., 2011; Larson et al., 2012; Albrecht et al., 2017; Dimitriou et al., 2018; Hillestad et al., 2018; Qin et al., 2018; Michailos and Bridgwater, 2019). Here, the gasifier is operated at 1,300°C and 25 bar. At this temperature, the volatile matter in the biomass completely breaks into gaseous products, which means that an additional tar cracking unit is unnecessary (Swanson et al., 2010; Villanueva Perales et al., 2011; Albrecht et al., 2017; Dimitriou et al., 2018; Hillestad et al., 2018; Michailos and Bridgwater, 2019). Furthermore, ash is melted and recovered as liquid slags due to the high temperature. This reduces the gas cleaning requirement in the downstream application.

The EF-gasifier is modeled as an adiabatic Gibb's reactor operating at 1,300°C and 25 bar. For Case I and II, oxygen (99.5% purity) from the air separation unit (ASU) and for cases with SOEC integration, pure O_2 from the SOEC is fed to maintain the auto-thermal temperature of 1,300°C. Due to higher pressure in the gasifier, the biomass is fed to the EF-gasifier *via* a lock-hopper mechanism. The energy requirement for operating the lock-hopper mechanism is 0.082 kW per dry tons per hour of biomass (Swanson, 2009). The energy requirement for different processes is summarized in supporting information H.3. In addition to the biomass, the tail gas out of the FT reactors is also recycled back to the gasifier. The tail gas is heated to 400°C utilizing hot effluent gas out of the WGS reactor (Case I and II) and waste heat boiler (WHB) (Case III-VI).

In Aspen Plus modeling, biomass gasification is modeled as two steps process. First, the biomass decomposes to its elemental form and ash, modeled as a pyrolysis process in a yield reactor. The decomposition reaction is endothermic and is shown in Eq. 2 (Putta et al., 2022), where stoichiometric coefficients are calculated as $\nu_i = \frac{(\frac{w_i}{100})}{MW_i} MW_{\text{Biomass}}$.

$$C_{4.31}H_{6.0}O_{2.62}N_{0.012}S_{0.002}\,(\text{Biomass}) \rightarrow 4.31C + 3.0H_2 + 1.31O_2 + 0.006N_2 + 0.002S \quad (2)$$

Equation 2 also consists of ash The second step is modeled as a Gibbs reactor, where oxygen flow is controlled to maintain the reactor's temperature to 1,300°C. Since the temperature is very high, it is assumed that the gasifier behaves as an ideal Gibbs reactor where all the reactions are at an equilibrium. The Gibbs reactor block in Aspen Plus models the gasifier by the method of Gibbs free energy minimization. The second step is the oxidation of the elemental forms to CO, CO_2, and H_2O with several other gaseous by-products. The oxidation produces sufficient thermal energy to raise the temperature of volatiles from 250°C to 1,300°C. Although heat losses to the surrounding can occur, the heat loss is small for a large gasifier and is neglected here. In the case of Ash, it is removed at the decomposition temperature of 600°C. There is a discrepancy in the actual vs. simulated process, i.e., ash is removed at 1,300°C in the actual process while it is removed at 600°C in the simulated process. The discrepancy amounts to less than 0.04 MW (ca. 0.08%) and is neglected here.

A simplified gasification process is shown in Figure 3. The RWGS process in the figure only applies to Case III and IV. For those cases, H_2 from SOEC is fed to achieve high-temperature reverse water gas shift (RWGS) effects. The process is modeled as an equilibrium reaction. The RWGS reaction is shown in Eq. 3.

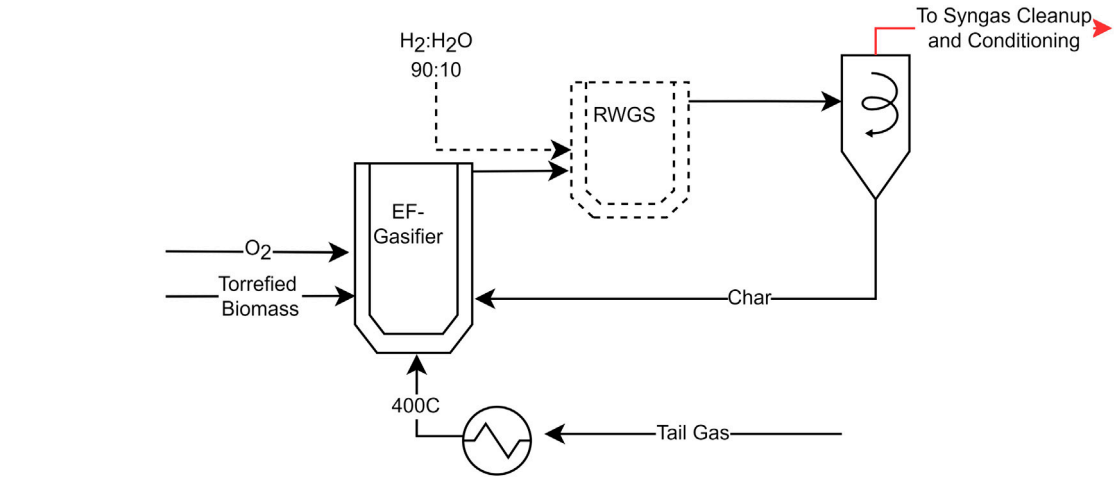

FIGURE 3
Block diagram of the biomass gasification process.

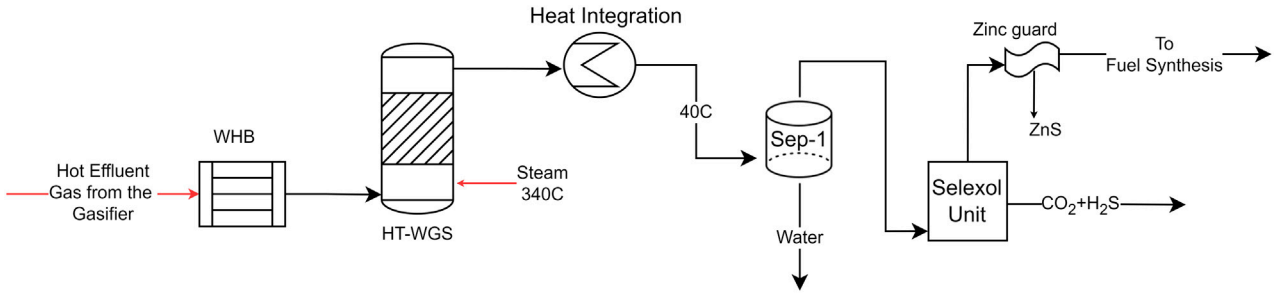

FIGURE 4
Block diagram for Syngas clean-up and conditioning in Case I and II. Heat integration here refers to the utilization of energy available in the hot effluent gas for heating O_2 from ASU (Case I and II), heating recycled tail gas to 400°C before it is fed to the gasifier (all cases). For Case III-VI, the excess heat is utilized to prepare the boiler feed water for WHB.

TABLE 1 Applicable process steps for Case I–VI in syngas clean-up and conditioning.

	Case I	Case II	Case III	Case IV	Case V	Case VI
WHB	Yes	Yes	Yes	Yes	Yes	Yes
HT-WGS	Yes	Yes	No	No	No	No
HX-2 (Process heat integration)	Yes	Yes	Yes	Yes	Yes	Yes
Sep-1	Yes	Yes	Yes	Yes	Yes	Yes
Selexol process	Yes	Yes	No	Yes	No	Yes
Zinc guard	Yes	Yes	Yes	Yes	Yes	Yes

$$CO_2 + H_2 \leftrightarrow CO + H_2O \quad (3)$$

In Case III and IV, hydrogen flow to the RWGS process is controlled to maintain an H_2/CO ratio of 1.7 in the 1st stage of FT synthesis. In the RWGS process, a fraction of the hydrogen is consumed to convert CO_2 to CO, while most of the hydrogen contributes to the increase in H_2/CO ratio in the syngas from ca. 0.6 to 1.7.

3.4 Gas clean-up and conditioning

Gas clean-up and conditioning are necessary to avoid poisoning the FT synthesis catalyst and maintain the appropriate syngas quality (Neuling and Kaltschmitt, 2018; Kargbo et al., 2021). The quality refers to syngas' desirable H_2/CO ratio and CO_2 composition. The generalized block diagram of gas clean-up and conditioning is shown in Figure 4. The diagram is strictly applicable for Case I and II. For novel BtL process concepts (Case III and IV), the appropriate process steps are summarized in Table 1.

The first conditioning steps include cooling the hot product gas out of the gasifier to 600°C or lower so that the product gas is thermo-chemically stable. This is carried out in the waste heat boiler. For Case I and Case II, the energy is used to produce superheated steam at 340°C for the WGS reaction. For Case III-VI, the entire energy is used to produce superheated steam at 40 bar and 750°C, which is utilized in the SOEC. After WHB, further gas cleaning is performed by passing the gas through the cyclone separator, where the char and flue ash are separated and recycled back to the gasifier. Finally, the gas is passed through a series of economizers and heat exchangers before being fed to the WGS reactor (applicable to Case I and II). The WGS reaction is shown in Eq. 1. The WGS is operated at 340°C, and the reactor is modeled as an equilibrium reactor operating under adiabatic conditions. This step produces excess CO_2 and will accumulate in the system if the gas is directly fed to the FT synthesis. To avoid this, the gas is cooled down, and CO_2 is removed in the acid gas removal unit. This study considers selexol unit for acid gas removal, and the data are acquired from the published literature (Hamelinck, 2004; Hillestad et al., 2018). The selexol unit is also helpful in reducing H_2S and COS concentrations in the syngas (Dieterich et al., 2020).

As seen in Table 1, the selexol process is incorporated in Case I, II, IV, and VI, while in Case III and V, the excess CO_2 remains in the system. In Case III and V, the excess CO_2 is purged or converted to CO in the gasifier. In Case III, the conversion also takes place in the RWGS unit. For cases with a selexol unit, 99% of the sulfur is removed in the selexol unit (Case I, II, IV, and VI), while 1% sulfur is removed in a zinc guard. For Case III and V, all sulfur is removed in the zinc guard. The idea is to reduce the H_2S and COS concentration to below 50 ppb (Swanson, 2009), which is critical for avoiding catalyst poisoning in FT synthesis.

3.5 The fischer-tropsch synthesis

The Fischer-Tropsch (FT) synthesis is a surface polymerization reaction, where hydrogen and CO polymerize to long-chained hydrocarbons. This study considers low-temperature Fischer-Tropsch operating between 200 and 225 °C over a cobalt catalyst. The products are primarily long-chain paraffins which favor a higher diesel/jet fuel yield following subsequent refining (Dry, 2002; Neuling and Kaltschmitt, 2018). The overall reaction in FT synthesis is shown in Eq. 4.

$$CO + UH_2 \rightarrow \nu_1 C_1 + \nu_2 C_2 + \nu_3 C_3 + \ldots + \nu_i C_i + H_2O \qquad (4)$$

The stoichiometric coefficient (ν_i) follows the Anderson Schulz-Flory (ASF) distribution with a growth parameter (α). The details on modeling FT products that follow the ASF distribution can be found in (Hillestad, 2015). The product consists of an infinite number of components, and lumping of the higher chain is required to adequately define the polymerization reaction. The details on modeling FT products with lumping, which follows the ASF distribution, can be found in (Hillestad, 2015). A model developed by Pandey et al. (2021) was used in the current study to describe the reaction kinetics and product distribution for the cobalt-based LTFT synthesis. The model lumps higher products to a hypothetical hydrocarbon component with variable molecular weight at a different section in the reactor. The average molecular weight and stoichiometric ratio for the lump varies with the temperature and H_2/CO ratio. Aspen Plus lacks the possibility of defining a pseudo-component with variable molecular weight. So, it is difficult to directly implement the model Pandey et al. (2021) developed in flowsheeting programs such as Aspen Plus.

Here, a customization tool available in Aspen Plus is utilized to incorporate a detailed kinetic model and simulate the fixed bed reactors employed in FT synthesis. The kinetic model is formulated in FORTRAN and then integrated into the Aspen Plus models. Five paraffin lumps and three olefin lumps with constant molecular weight are defined to address the issue with the lumps in Aspen Plus. The molecular weight for the lumps with constant molecular weight corresponds to the growth parameter of 0.93 and utilizes the lumping procedure described by Hillestad (2015). The rate of formation for each component is then evaluated in the FORTRAN program. The rate of formation of lumps with variable molecular weight is then assigned to the rate of formation with constant molecular weight using the molecular weight ratio as a correction factor. This helps formulate a "closed" product distribution model that incorporates all possible products in the lumps.

A typical two-stage FT synthesis modeled in this study is shown in Figure 5. The figure demonstrates the fuel synthesis for Case V. For other Cases, the process steps applicable for different cases are summarized in Table 2.

The fuel synthesis in the conventional BtL process concepts (Case I and Case II) consists of a single-stage, while all the novel processes consist of two-stage FT synthesis. In Case I, the feed H_2/CO ratio is set to 2.05 with the per pass CO conversion of 40%. The tail gas is recycled back to the gasifier, and a fraction of the tail gas is purged out. Purge flow is adjusted to maintain the makeup gas's N_2 mole fraction lower than 5 mol%.

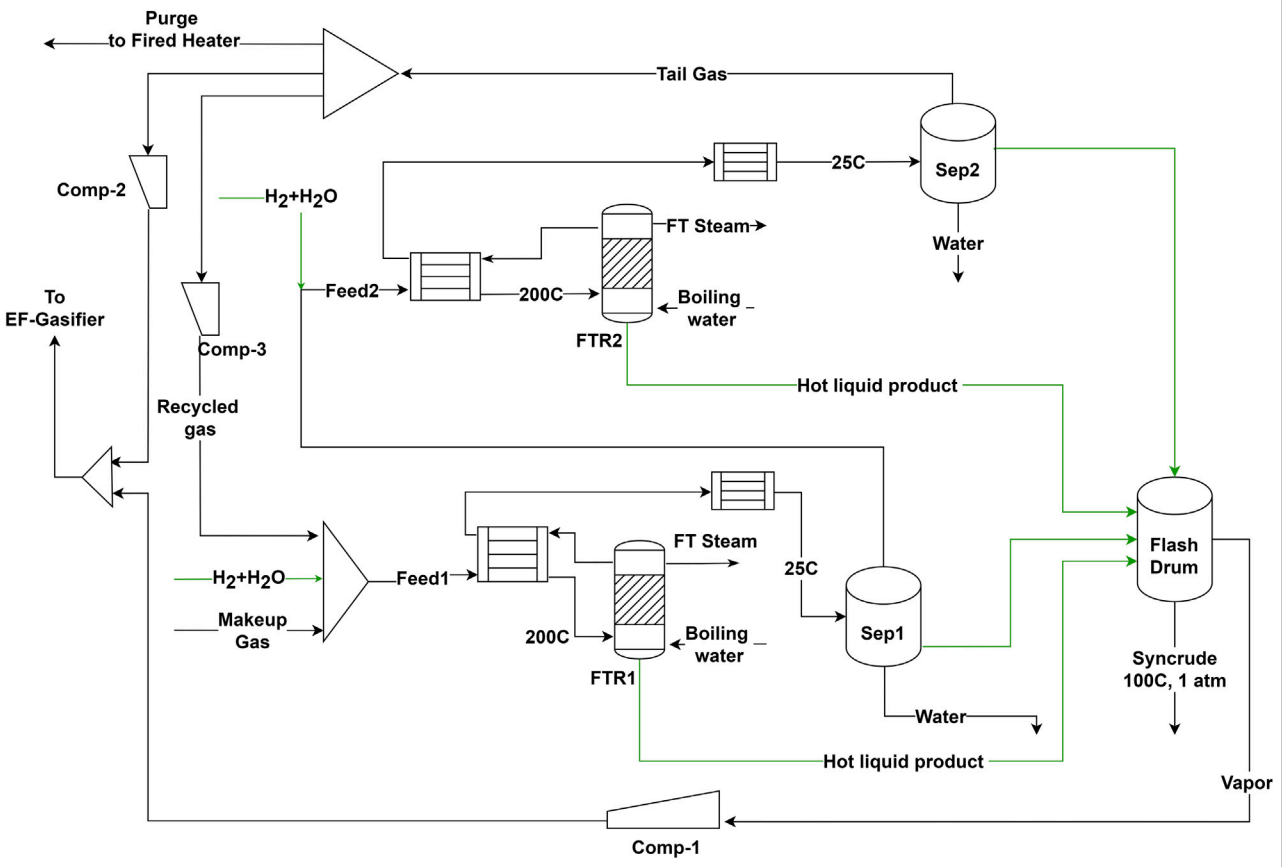

FIGURE 5
Process flow diagram of fuel synthesis process in Case V.

TABLE 2 Process steps applicable for different Cases in the fuel synthesis process.

	Case I	Case II	Case III	Case IV	Case V	Case VI
Number of stages	1	1	2	2	2	2
SOEC H_2 feeding to 1st stage	No	No	No	No	Yes	Yes
SOEC H_2 feeding to 2nd Stage	No	No	Yes	Yes	Yes	Yes
Internal recycling of tail gas to 1st Stage	No	Yes	Yes	Yes	Yes	Yes
H_2/CO ratio in the reactor feed	2.05	1.7	1.7	1.7	1.7	1.7
Per pass stage conversion	40%	60%	60%	60%	60%	60%

For all other cases, the H_2/CO ratio in the reactor feed is maintained at 1.7, and per pass CO conversion over a stage is set to 60%. Internal tail gas recycling from the final stage to the first stage FT reactors (FTR1) is introduced for all the cases. The recycle to makeup gas ratio is adjusted to maintain an N_2 mole fraction lower than 10% in reactor feed to the FTR1. In the Case of novel BtL processes, the fuel synthesis section also consists of feeding the H_2 to the second stage FT reactors (FTR2). In Case V and VI (direct H_2 feeding process concepts), H_2 is fed to FTR1 to maintain a desirable H_2/CO ratio of 1.7. The feed gas is heated to 200°C before it is fed to the FT reactors, where it reacts to produce FT products. The product consists of hot liquid and vapor. The vapor is heat exchanged with the reactor feed and cooled down to 25°C. It is then fed to a 3-phase separator (3-Sep1) which separates it into tail gas, light products, and water. The light products are mixed with hot liquid products and flashed into a storage drum maintained at 1 bar and 100°C. The idea here is to maintain the liquid form, which could be easily transported to the

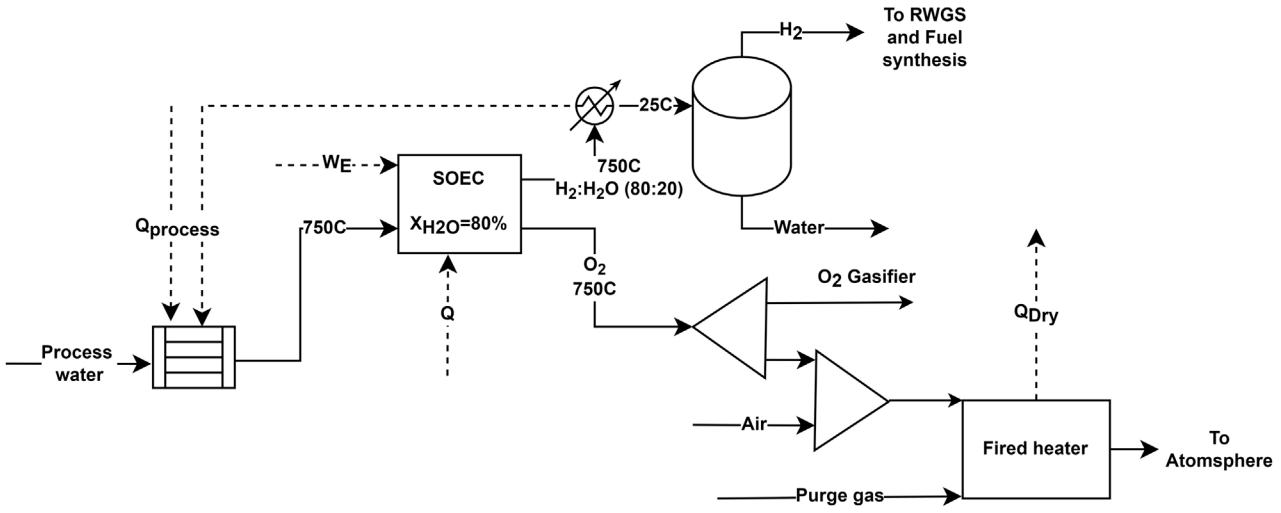

FIGURE 6
Block flow diagram of the SOEC model. Heat integration includes WHB and heat economizers, which utilize the heat in the hot effluent gas.

external refineries. The light tail gas is either recycled back to the EF-gasifier (Case I), recycled back to FTR1 (Case II), or fed to FTR2 (Case III, IV, V, and VI). Some fraction of tail gas is purged out as per the design criterion of N_2 mole fraction.

This study considers fixed bed FT reactors for fuel synthesis in FTR1 and FTR2. Heat transfer is a critical factor in the design of FT reactors, especially fixed bed reactors. The current study considers reactor tubes of 1-inch diameter and 10 m in length, and the overall heat transfer rate is assumed to be 400 W/m^{2}K. The value here is similar to the one used in the same author's optimization study of FT synthesis (Pandey et al., 2022). In addition, the recommendation of the optimization study is utilized in the current study to achieve improved performance over the FT synthesis. In addition to the parameters mentioned in Table 2, the optimized process parameters employed in Case II-VI are: internal recycle adjusted to achieve 96.1% overall CO conversion for Case III-VI and 69.9% for Case II, and coolant temperature set to 210.6°C. As a result, the H_2/CO ratio here is slightly under stoichiometric, favoring the production of valuable products (syncrude) without accelerating the degradation of the cobalt catalysts.

3.6 Air separation unit and solid oxide electrolyzer cell model

Oxygen with 95% or higher purity is used in biomass gasification in an EF-gasifier (Swanson et al., 2010; Villanueva Perales et al., 2011; Larson et al., 2012; Albrecht et al., 2017; Dimitriou et al., 2018; Hillestad et al., 2018; Qin et al., 2018; Michailos and Bridgwater, 2019). Here, oxygen flow maintains the EF-gasifier temperature to ca. 1,300°C. For Case I and II, an ASU is incorporated to produce 99.5% pure oxygen, while for other cases with SOEC integration, O_2 produced from the electrolysis is directly utilized. In the Aspen Plus modeling, ASU is modeled as a black-box model. Previous studies have shown that it is an energy-intensive and costly component in a typical gasification-based process, especially in small-scale BtL plants (Tijmensen et al., 2002; Swanson, 2009; Hillestad et al., 2018). The cost increases with the increase in the purity of oxygen. Nevertheless, it is important to feed pure or almost pure oxygen to avoid producing a high concentration of nitrogenous products and reduce the size of the downstream equipment. The energy requirement for the ASU is 420 kWh/ton-O_2, including an air compressor and auxiliaries (James et al., 2019).

Like ASU, SOEC is modeled as a black-box model. The typical operating condition for the SOEC is 700°C–1,000°C and 1–15 bar pressure (Keçebaş et al., 2019). However, for the process to be applicable for the BtL process, the operating pressure should be at least higher than the gasifier pressure. Hillestad et al. (2018) have suggested operating the SOEC at elevated pressure by keeping it inside a pressure vessel, thus reducing the shear stress in the SOEC material walls. This study assumes that future SOEC units can operate at an elevated pressure of 40 bar and be commercially available. The block diagram of the black-box SOEC model is shown in Figure 6. The heat demand in the SOEC is given by $Q = T\Delta S$. Based on the operating condition, three operating modes exist in the electrolytic process:

TABLE 3 Key technical results of the simulation in EF-gasifier.

	Case I	Case II	Case III	Case IV	Case V	Case VI
H_2/CO ratio in the effluent gas out of the gasifier	1.26	0.85	0.64	0.73	0.50	0.70
CO_2 removed in selexol unit (kmol/h)	214.7	171.2		34.0		46.3
CO_2 conversion in RWGS process			32.3%	27.7%		
CO_2 mole fraction in makeup syngas	0.013	0.017	0.036	0.001	0.14	0.007
CO_2 mole fraction in gas out of RWGS			0.032	0.025		
CO_2 mole fraction in the effluent gas out of the gasifier	0.013	0.003	0.076	0.054	0.12	0.057
H_2 produced in the SOEC (kmol/h)			748.0	624.2	733.0	576.4
H_2 added to the RWGS unit (kmol/h)			615.4	506.1		
H_2S + COS in effluent gas out of the gasifier (ppmv)	14.8	27.3	30.4	21.3	29.4	33.3
External recycle to makeup gas ratio (kg/kg)	0.67	0.44	0.21	0.14	0.34	0.14
External recycle to dry biomass feed ratio (kg/kg)	1.50	0.62	0.39	0.20	0.67	0.19

TABLE 4 Electrical power consumption in different process units and FT synthesis simulation results for different cases.

	Case I	Case II	Case III	Case IV	Case V	Case VI
Compressor duty (kW)	469.3	128.7	208.7	169.7	244.9	116.7
Pump duty (kW)	4.92	6.99	32.6	27.7	32.8	26.2
ASU duty (kW)	1852.0	1,147.0				
SOEC electrical duty (kW)			51,669	35,500	50,635	39,800
Selexol electricity consumption (kW)	537.9	446.7		85.1		
Grinder electrical duty (kW)	1855.7	1855.7	1855.7	1855.7	1855.7	1855.7
Lock hopper electrical duty (kW)	19.7	19.7	19.7	19.7	19.7	19.7
FT synthesis						
H_2 added to the 1st Stage (kmol/h)					604.8	460.2
H_2 added to the 2nd Stage (kmol/h)			132.6	83.7	128.2	116.2
Overall CO conversion (%)	40.0	69.9	96.1	96.1	96.1	96.1
Internal recycle to makeup gas ratio		0.231	0.838	0.529	1.35	0.57
Number of FT reactor tubes	1873	3,107	5,145	4,658	5,085	4,612
Purge to makeup gas ratio	0.016	0.014	0.018	0.007	0.024	0.018
LHV syncrude (MJ/kg)	42.8	42.7	42.8	42.8	42.8	42.8
Syncrude production (bbl/h)	26.7	32.1	56.5	53.6	56.1	50.2
Syncrude compositions						
C_1-C_4	0.001	0.004	0.003	0.009	0.003	0.004
C_5-C_{12}	0.220	0.256	0.237	0.264	0.235	0.235
C_{13}-C_{23}	0.369	0.341	0.357	0.341	0.357	0.358
C_{24+}	0.408	0.394	0.401	0.382	0.403	0.401
H_2O	0.002	0.006	0.001	0.004	0.001	0.002

exothermic mode, thermoneutral mode, and endothermic mode (Hillestad et al., 2018). In an exothermic mode, the ohmic resistance is significant, and the electric work (W_E) exceeds Gibbs free energy of formation of compound (ΔG) for the electrolysis. As a result, the electrical efficiency becomes lower than 100%.

Conversely, the ohmic resistance becomes negligible at high temperatures, and the process becomes endothermic. This reduces the overall electrical load, and the process achieves "super efficiency", or the electrical efficiency becomes higher than 100%. In the thermoneutral mode, the efficiency is 100% meaning the electrical energy requirement is the same as the

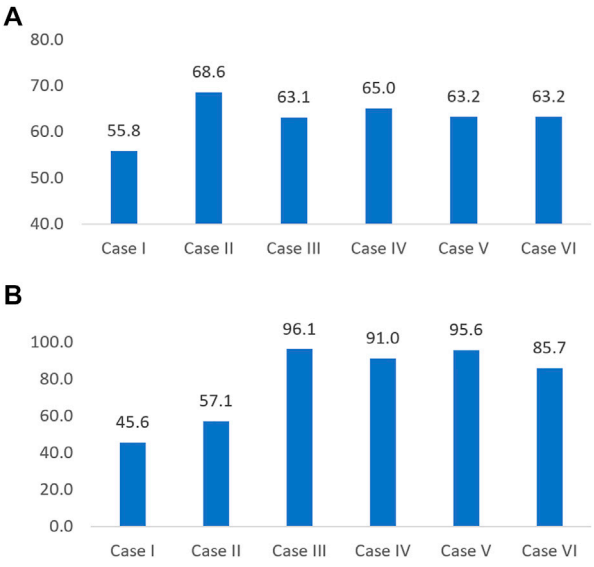

FIGURE 7
(A) Energy efficiency and **(B)** carbon efficiency in Case I–VI.

Gibbs free energy (ΔG). The relationship between W, Q, and ΔG is given by Eq. 5.

$$W_E = \Delta G + Q \tag{5}$$

Here, we assume a thermoneutral mode of operation where the product exit at the same temperature (750°C) as the feed temperature (750°C). The steam conversion is 80%, meaning 80% of H_2O splits into H_2 and O_2. The unconverted H_2O exits with H_2 in the cathode. The moist H_2 is cooled down and dried before being utilized in RWGS and fuel synthesis. In Case III and IV, a fraction of dry H_2 is heated to 500°C before being fed to the RWGS unit. The remaining fraction is mixed with the feed gas in the second stage of FT synthesis to achieve a desirable H_2/CO ratio. For Case V and VI, the dry H_2 is directly mixed with the feed gases in either of the stages to achieve a desirable H_2/CO ratio in the feed gas. The cost data for SOEC operating in thermoneutral mode at 750°C is obtained from the techno-economic study by Mýrdal et al. (2016). The study estimated the SOEC cost to be $1,059/kW installed and the stack replacement cost to be $448/kW. This study assumes that the SOEC stacks are replaced every 2 years.

4 Technical indicators

4.1 Process results

The key technical results of the simulation of an EF-gasification model, ASU/SOEC model, and syngas clean-up and upgrading are shown in Table 3. The H_2/CO ratio out of the gasifier is ca. 0.6~0.7 for novel BtL processes, while the value is much higher for Case I. The huge recycling of H_2-rich tail gas contributes to the higher H_2/CO ratio for Case I. In other cases, the recycled tail gas is much lower than the biomass feed. This reduces the H_2/CO ratio in the gas out of the gasifier. The operating H_2/CO for FT synthesis, as described in Table 2, is maintained by the WGS reaction for Case I and II. In the WGS, 212.8 kmol/h (27% CO conversion) and 186.8 kmol/h (33.6% CO conversion) of CO are converted to CO_2 in Case I and II, respectively. After the WGS, the H_2/CO ratio is 2.05 and 1.7, respectively. The excess CO_2, 214.7 kmol/h for Case I and 134.6 kmol/h, are removed in a selexol unit. For cases with the RWGS unit (Case III and Case IV), 615.4 kmol/h and 488.7 kmol/h of H_2 are added to the RWGS unit to achieve 32.3 and 27.7% of CO_2 conversion to CO, respectively. This reduces the CO_2 mole fraction from 0.08 to 0.03 and 0.05 to 0.03. This shows that the impact of the RWGS unit is minimal, and the CO_2 concentration in the gas out of the gasifier is already very low.

The electrical power consumption for the different subprocesses and results for fuel synthesis is shown in Table 4. For a BtL plant of 51.4 MW (LHV), the electrical consumption varies with the type of process. For novel BtL processes, the electrical load is mostly in SOEC. Case III corresponds to the highest electrical energy consumption among the novel BtL cases. The energy is lower for other novel BtL cases (Case IV, V, and VI) as a higher proportion of carbon is lost as CO_2 in the process. Among the two conventional-BtL processes, Case II has a lower total electrical load. The saving comes mostly in ASU as the overall demand for the O_2 in the gasifier for Case II is lower due to reduced overall material flows compared to Case I.

The overall CO conversion is maintained at 96.1% by introducing internal recycling from the 2nd to the 1st stage for Case III-VI. Among the novel process concepts, the internal recycle to makeup gas ratio is below 1 for Case III, IV, and VI. At the same time, it is higher than 1 for Case V. Lack of RWGS integration and recycling of excess CO_2 removal means that the overall material flows are much higher, as demonstrated by the internal recycle to makeup gas ratio. The syncrude production varies between 26.7 and 56.5 bbl/h. The highest production is achieved for Case III, where 96.1% of carbon in the biomass ends up as a valuable product, while the number is only 45.6% for Case I. The estimated lower heating value (LHV) of syncrude is similar to a typical diesel/jet fuel. The syncrude primarily consists of C_5 and higher products. The share of heavier products (C_{24+}) is approximately 40% of syncrude for all the cases.

4.2 Process efficiencies

Two different process efficiencies are used to evaluate the performance of a BtL process: energy efficiency and carbon

TABLE 5 Cost data used in the techno-economic analysis.

Equipment	Base cost ($M)	Base size (S_0)	Scale factor (n)	Installation factor (f_{inst})	Base year	References
Feeding system	0.48[a]	33.5 wtph	1	2	2002	Hamelinck (2004)
Conveyors	0.41[a]	33.5 wtph	0.8	2	2002	Hamelinck (2004)
Rotary dryer	6.337[a]	18.55 tph moisture	0.79	2.4	2007	Swanson (2009)
Grinder	0.668[a]	92.6 tph dry biomass	0.49	2.63	2007	Swanson (2009)
Storage	1.05	33.5 tph wet biomass	0.65	2	2007	Hamelinck (2004)
ASU	57	53.7 tph O_2	0.7	1	2018	Hillestad et al. (2018)
EF-gasifier with lock hopper	23.2	17.2 dtph	0.7	2.48	2007	Reed and Bibber (2007)
EF-gasifier with RWGS	254.9	435 MW (LHV biomass)	0.7	1	2018	Hillestad et al. (2018)
Cyclones	3	34.2 m^3/s	0.7	2	2002	Hamelinck (2004)
WHB and BFW system	47.4	435 MW (LHV biomass)	0.6	1	2018	Hillestad et al. (2018)
WGS reactor	12.2	8,819 kmol/hr of CO + H_2	0.65	1.81	2002	Hamelinck (2004)
Selexol CO_2 removal	63	9,909 kmol CO_2/hr. (90% CO_2 removal)	0.7	1	2002	Hamelinck (2004)
Guard bed	0.024	8 NTP m^3/s gas	1	3	2002	Hamelinck (2004)
FTR	7.3	180.756 m^3	0.72	3.6	2007	Swanson (2009)
Fired heater	8.54	24.6 Mw	0.6	1	2019	Rezaei and Dzuryk (2019)
Heat exchangers, separators, pumps, compressors	Aspen capital cost estimator					

[a]Means M€ instead of M$.

efficiency. The energy efficiency indicates the capacity of the process concept to convert input energy into valuable products, and carbon efficiency indicates the capacity to retain carbon in the biomass feed in the syncrude.

4.2.1 Energy efficiency

The energy efficiency is calculated as shown in Eq. 6. Here, W is an electrical work in the process. For novel BtL process concepts, the contribution of electrical work to the total input energy to the process is as high as 51.1%.

$$\eta_e = \frac{\dot{m}_{C,\,syncrude} LHV_{syncrude}}{\dot{m}_{C,Biomass} LHV_{Biomass} + W} \quad (6)$$

The energy efficiency for different cases is shown in Figure 7A. The energy efficiency is the highest for Case II and the lowest for Case I. Among the novel BtL process concepts, Case IV and Case VI with the CO_2 removal process have marginally better energy efficiency than their counterparts Case III and Case V, respectively. In both cases, the total thermal energy retained in syncrude ($\dot{m}_{syncrude} LHV_{syncrude}$) is improved with the recycling of the excess CO_2, but the electrical work (W_E) in the SOEC is much higher, resulting in lower energy efficiency.

4.2.2 Carbon efficiency

The carbon efficiency is calculated using Eq. 7. The carbon efficiency for different cases is shown in Figure 7B.

$$\eta_C = \frac{\dot{m}_{C,\,syncrude}}{\dot{m}_{C,Biomass}} \quad (7)$$

The carbon efficiency for conventional BtL (Case I) is 45.6%. The efficiency could be increased to 57.1% (Case II) by operating at optimal process conditions, as suggested by Pandey et al. (2022). Case III has the highest carbon efficiency among the novel BtL process concepts. The addition of H_2 along with the recycling of excess CO_2 helps to achieve as high as ca. 96% carbon efficiency in Case III and V. The integration of RWGS in Case III marginally improves the carbon efficiency in Case III compared to Case V. For Case IV and VI, the additional CO_2 removal process lowers the carbon efficiency as 8% and 11% of carbon is lost as CO_2 in the selexol unit, respectively.

5 Economic analysis

A discounted cash flow is formulated, and economic analysis is performed for all the process concepts. The economic criterion used for the analysis is summarized in the supporting information H.1. The economic analysis calculates the minimum selling price (MSP) of syncrude for different cases and compares the economic viability of different process concepts. Further, the effect of electricity prices and SOEC costs in the MSPs of syncrude is studied to evaluate the

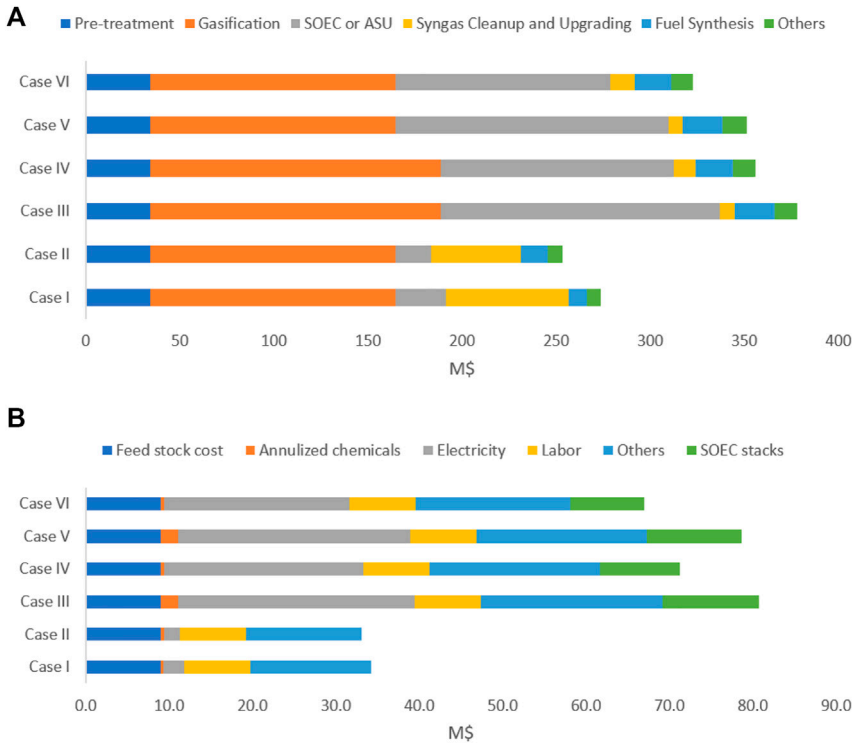

FIGURE 8
(A) CAPEX and **(B)** OPEX breakdown for different Cases.

economic viability of the BtL processes for different cost scenarios.

5.1 Capital expenditure

The estimation of capital expenditure (CAPEX) is conducted for "n th-plant" as most of the technology discussed here, except SOEC technology, is available on a commercial scale. The scaling component method is used to determine the installed equipment cost, as shown in Eq. 8 (Sinnott and Towler, 2019). The cost of the equipment in the base year ($C_{\text{eq,Base year}}$) and empirical scaling factor (n), were extracted from the published works of literature and are summarized in Table 5. The details on the calculation of CAPEX are given in supporting information I.3. The Aspen Icarus Capital Cost estimator is used to estimate the total installed cost for the heat exchangers, separators, compressors, and pumps.

$$C_{\text{eq, Base year}} = C_{0,\text{Base year}} \times \left(\frac{S}{S_0}\right)^n \tag{8}$$

The CAPEX results and the CAPEX breakdown are shown in Figure 8A. The figure shows that the gasifier is a major investment cost for a BtL process. The EF-gasifier accounts for 37%–51% of the CAPEX. For conventional BtL processes (Case I and II), the syngas clean-up and upgrading are significant investments where the water-gas shift process and selexol unit are two critical processes. For novel BtL processes (Case III-IV), the SOEC is equally crucial as the EF-gasifier.

The figure shows that the conventional BtL processes (Case I and II) have a lower total investment cost. The CAPEX for Case II with optimal fuel synthesis is even lower than Case I. Between conventional process concepts (Case I and II), Case I has higher overall material flows due to a lack of internal recycling across the fuel synthesis and lower CO conversion. This increases the overall load in the WGS reactor and the selexol unit compared to Case II and the total investment cost contribution from the syngas clean-up and upgrading process. Although the investment cost in fuel synthesis is higher for Case II, the higher capital cost in syngas clean-up and upgrading eclipses the lower cost in the fuel synthesis in Case I. The SOEC is a major investment in Case III-VI, with SOEC accounting for 35%–42% of the total capital investment. The CAPEX is highest for Case III due to two factors: higher load in SOEC and integration of RWGS process. The future improvement in the cost of SOEC, as predicted by Mýrdal et al. (2016), would greatly impact the economic viability, as seen in Figure 8A.

TABLE 6 Summary of economic analysis for different cases.

Description	Case I	Case II	Case III	Case IV	Case V	Case VI
CAPEX (M$)	273.5	253.5	378.1	356.1	351.5	322.8
Annualized OPEX (M$)	34.3	33.1	80.8	71.3	78.6	67.0
Revenues (M$)	76.5	72.5	137.9	125.3	131.6	116.0
Syncrude MSP ($/L)	2.17	1.73	1.90	1.82	1.82	1.79

5.2 Operating expenditure and revenues

In a BtL plant, the OPEX consists of the cost associated with purchasing feedstocks, chemicals, and utilities, electrical costs, labor costs, administrative services, maintenance, and insurance and taxes. Labor costs are divided into salaries and overhead costs associated with the operators, maintenance technicians, engineers, and other management employees. The number of operators for a fully automated process can be estimated using Eq. 9 (Turton et al., 2008). The details on the labor cost estimation can be found in the supporting information I.2.

$$N_{OL} = \left(6.29 + 31.7P^2 + 0.23N_{np}\right)^{0.5} \quad (9)$$

The cost of utilities and chemicals considered in the techno-economic analysis are summarized in the supporting information H.2. The cost of the consumables and utilities has been adjusted to the year 2022 using the CEPCI index. The maintenance cost was assumed to be 2% of the CAPEX, administrative services 1% of CAPEX, and insurance and taxes 2% of the CAPEX. For the novel BtL process, SOEC stack replacement cost also accounts for the OPEX. Mýrdal et al. (2016) estimate the replacement cost of $448/kW.

The OPEX and breakdown of the OPEX are shown in Figure 8B. For conventional BtL processes, feedstock, and indirect costs (maintenance, administrative, insurance, and taxes) are significant contributors. Case II has slightly lower operating costs than Case I. The saving in operating costs is primarily in the selexol unit and ASU. For novel BtL processes with SOEC integration (Case III-Case VI), the electrical cost is the most significant contributor to the OPEX. SOEC stacks and total electrical costs account for 46%–51% of the total OPEX. The OPEX is higher for Case III and IV indicating that more electrical energy is needed to achieve carbon efficiency as high as 96%. Conversely, the OPEX is lower for Case IV and VI as removing excess CO_2 lowers the electrical demand and SOEC replacement costs.

For the revenues, the products are assumed to be sold as a syncrude which then could be utilized in existing petroleum refining technologies and produce jet fuel. Syncrude costs vary to calculate the minimum selling price (MSP). In addition to jet fuel, steam is available as a commercial product. It is assumed that the steam can be sold in the market. The price of steam is calculated as suggested by Sinnott and Towler (2019). It can be found in the supporting information I.1. The steam price is estimated to be $19.2/MWh for high-quality saturated steam (300°C) and $14.9/MWh for low-quality FT steam (210.6°C). For Case I and II, high-quality and low-quality steam are available. For Case III-VI, only medium pressure FT steam is available. For all the cases, the revenues from the syncrude constitute more than 96%, and additional revenues from selling steam have minimal impact on the techno-economic analysis.

5.3 Summary of economic analysis and minimum selling price of the syncrude

The summary of the techno-economic analysis is shown in Table 6. Minimum selling prices (MSPs) are calculated for all the cases using the economic criterion mentioned in supporting information H.1. The analysis shows that the novel BtL process concepts (Case III-VI) have lower MSPs than conventional concepts. Among the conventional concepts, implementing optimal fuel synthesis design improves the minimum selling price by 25.4%. The improvement results from the overall reduction in CAPEX, OPEX, and revenue from the syncrude sale. Case VI (direct H_2 utilization in fuel synthesis with selexol CO_2 removal unit) has the lowest MSP among the novel processes. For the considered electricity price and SOEC investment costs, the process concepts with selexol removal units perform better than their counterparts (Case III vs. IV and Case V vs. VI). However, the MSPs could vary drastically for Case III-VI if there are fluctuations in costs associated with SOEC (electrical energy and investment costs).

5.4 Effect of solid oxide electrolyzer cell costs and electricity prices

The economic analysis shows that the optimized conventional process concept (Case II) has the best economic viability among the different process concepts. Compared to Case

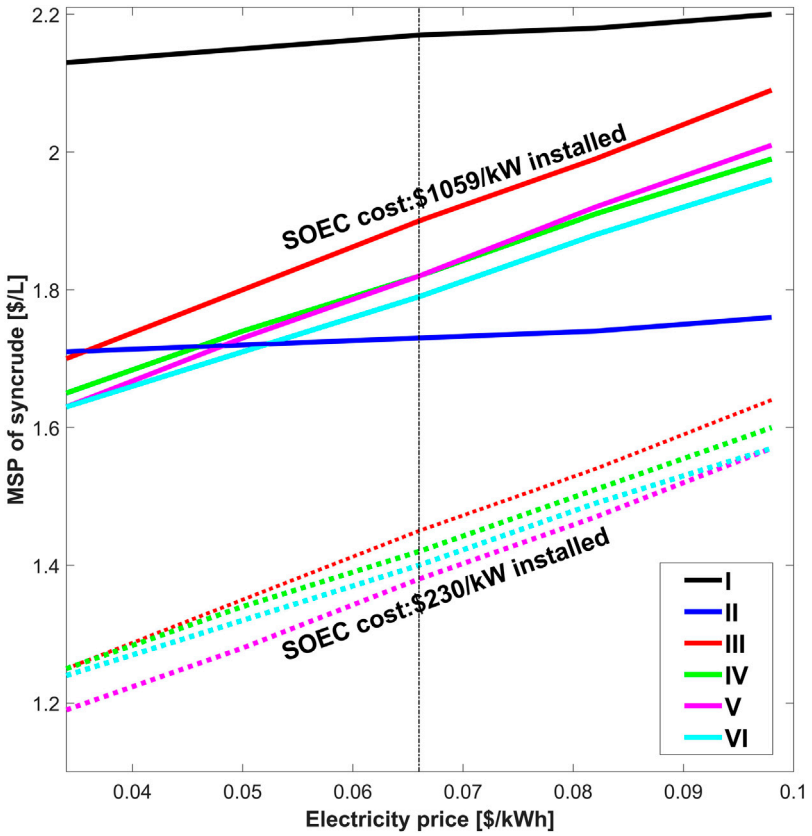

FIGURE 9
Effect of electricity prices and SOEC costs on MSPs of the syncrude. Here, the dotted line refers to MSPs estimated for SOEC installed cost of $230/kW and stack replacement cost of $52/kW for Case III-VI and solid lines refer to MSPs estimated for SOEC installed cost of $1,059/kW and stack replacement cost of $448/kW. The vertical dotted line refers to the electricity price of $0.066/kWh. The SOEC cost does not affect Case I and II.

II, the total syncrude production is almost 1.56–1.76 higher for novel BtL cases, and the novel BtL processes are able to maximize biofuel production from limited biomass resources. However, the increase in production comes at high SOEC costs and electricity prices which lowers the economic viability of the novel BtL plants. The SOEC replacement and electricity costs contribute as high as 51% of the total OPEX and 41% of the total CAPEX. Mýrdal et al. (2016) estimated the initial investment to be $1,059/kW and stack replacement cost to be $448/kW in 2020. The study predicts that the initial installed cost could drop as low as $230/kW and the stack replacement cost to drop to $52/kW with the maturing of the SOEC technology. The drop in prices could dramatically increase the viability of the novel BtL plants. Although the SOEC costs are likely to drop, the electricity price depends on the future energy market and is much more volatile. The effect of variation in electricity prices and its impact on the viability of novel BtL plant with present SOEC cost ($1,059/kW), as well as the futuristics cost of SOEC ($230/kW), is presented in Figure 9. The solid lines correspond to the variation in MSPs of syncrude with electricity prices for the current SOEC investment cost, while the dotted line corresponds to the variation in MSPs of syncrude for the futuristic cost of SOEC in novel BtL process concepts. The SOEC prices have no effects, while electricity prices have a negligible impact on MSPs of the syncrude for conventional BtL processes (Case I and II).

The figure shows that the price variation significantly impacts the syncrude MSPs for the novel BtL concepts (Case III-VI). For the electricity price and SOEC costs considered in the current stud, Case II has the lowest MSP and, subsequently, the best economic performance. The electricity prices need to drop below $0.052/kWh for the novel BtL process to outperform Case II. In this scenario, the MSPs for Case VI becomes the lowest among all the process concepts. Case VI has the best economic performance among the novel process concepts for electricity prices of ca. $0.040/kWh or higher. For a price of $0.040/kWh or lower, Case V becomes marginally better than all other process concepts.

For the futuristics SOEC costs ($230/kW installed cost and $52/kW stack replacement cost), all novel processes perform significantly better than Case I and II. For these SOEC costs, Case

V has the lowest MSP for all electricity prices. The MSP could drop to as low as $1.38/kWh (electricity price: $0.066/kWh) in Case V. Case V outperforms all other Cases even if the price of electricity is as high as $0.1/kWh. In all SOEC price scenarios, Case III and IV underperform compared to Case V and VI due to higher investment costs in RWGS units. The accrued cost with RWGS units is unable to overcome higher syncrude production even at favorable electricity prices and SOEC costs.

6 Discussion

The syncrude production is between 26.7 and 56.5 bbl/h for a biomass feed of 15.9 wtph. The syngas production increases with the addition of electrical energy in the SOEC, as suggested by a prior study (Putta et al., 2022). This also increases the total syncrude production and carbon efficiency as more carbon is retained in the syncrude. The novel BtL cases have carbon efficiency between 85.7% and 96.5%, while the conventional BtL process concept (Case I) has a carbon efficiency of 45.6%. The loss in carbon in the WGS reaction to achieve a stoichiometric H_2/CO ratio in the FT reactors results in the lower carbon efficiency in Case I. The carbon efficiency in conventional BtL could be improved from 45.6% to 57% by optimizing the operating H_2/CO ratio and recycle stream as in Case II. Case II performs better in terms of overall carbon efficiency and energy efficiency as well as the economic criterion. Lowering the operating H_2/CO ratio in the FT synthesis and introducing the internal recycle stream over the FT synthesis reduces the overall H_2 demand. This, in turn, reduces the loss of CO in the form of CO_2 in the WGS process. For the novel BtL processes, adding energy in the form of H_2 from SOEC is a critical factor in achieving higher carbon efficiency. The RWGS integration and recycling of excess CO_2 in Case III amounts to the highest carbon efficiency among all the cases, including the conventional concepts. The carbon efficiency is slightly lower for other cases than for Case III as higher carbon is lost as CO_2 either in the selexol unit (Case IV and VI) or in the purge.

The energy efficiency is highest for Case II (68.6%), while it is lowest for Case I (55.8%). Case II has two distinct advantages over other process concepts: optimized fuel synthesis design and lower overall material flows. The loss of input energy is inevitable in a BtL process due to the low hydrogen content in the biomass and thermal energy loss in low-quality heat. For Case II, the loss is lowest as the process concept employs optimized design to retain maximum possible input energy in the syncrude. In addition, the process has lower overall material flows, resulting in much lower O_2 demand in the EF-gasifier (4.41 tph for Case I and 2.73 tph for Case II) and CO_2 removal in the selexol unit (214.7 kmol/h in Case I and 171.2 kmol/h in Case II). As a result, the electrical duty of the ASU is reduced from 1.85 to 1.15 MW in the ASU and 0.54 to 0.45 MW when replacing conventional BtL (Case I) with the optimized conventional BtL (Case II) process. The lower overall material flow also reduces the loss of total low-quality thermal energy in cooling water from 6.75 to 5.1 MW between Case I and II. The novel BtL cases have significantly higher energy efficiencies than in Case I but lower than in Case II. Like Case II, higher conversion and optimized fuel synthesis design help achieve high energy efficiency in Case III-VI. However, the energy loss in cooling water is higher than in Case II, which results in slightly lower energy efficiencies for novel BtL process concepts. Among the novel BtL process concepts, Case IV, with removing excess CO_2, has the highest energy efficiency indicating a trade-off between carbon and energy efficiency.

The economic evaluation of different process concepts yields MSPs of syncrude between $1.73~2.17/L. The estimated MSPs for novel BtL plants with SOEC integration are slightly higher than the optimized conventional BtL plant (Case I) and significantly lower than the conventional BtL plants (Case I). The techno-economic analysis shows that directly utilizing hydrogen from the SOEC to maintain the H_2/CO ratio in the FT synthesis and removing excess CO_2 (Case VI) has the best economic performance among the novel process concepts. The MSP for Case V is $1.79/L which could drop to $1.38/L if the SOEC investment cost is greatly reduced from $1,059/kW installed to $230/kW. The SOEC investment costs account for 35%–42% of the total investment cost, and the stack replacement costs account for ca. 11% of the total operating costs. Thus, any variation in SOEC costs greatly affects the performance of the novel BtL plants. The effect of electricity prices is similar as it accounts for 31%–40% of the total OPEX for novel BtL process concepts.

The area of cost reduction in novel BtL process concepts lies in a possible drop in the electricity prices and SOEC costs with the maturing of technologies. In the case of a significant reduction in electricity prices or SOEC costs, novel BtL processes become economically more viable than conventional BtL processes. Case V performs best among the novel BtL process concepts in such scenarios. The major advantage of Case V over other cases lies in the possibility of maximizing the syncrude production by recycling excess CO_2 in the process. Although total syncrude production is highest for Case III, the modification in EF-Gasifier to incorporate an RWGS process is much more consequential in terms of the total capital investment costs. Consequently, Case V has lower MSPs than Case III for all electricity prices and SOEC cost scenarios. The MSP for novel process concepts increases significantly at high electricity prices or SOEC costs. The optimized conventional BtL process (Case II) becomes more cost-competitive in those price scenarios. Therefore, in high-cost scenarios, it is economically beneficial to reduce the load in SOEC by removing excess CO_2 (Case VI) or not operate the SOEC (Case II).

The estimated MSPs of syncrude in different cases are between $1.73~2.1/L. The values are significantly higher than the current crude oil price (WTI crude price of $0.66/L). The crude oil price was at an all-time high in 2008 at $0.88/L. The estimated price of a syncrude is still much higher than the all-

time high price of crude oil. In a very optimistic scenario, the SOEC investment cost could drop significantly, as suggested by Mýrdal et al. (2016). In that case, the MSPs of syncrude become $1.38/L which is still higher than the current crude oil prices. Comparing syncrude with crude oil is tricky as the upgrading cost of crude oil is much higher due to the presence of sulfur in the crude oil. Nevertheless, the price of jet fuel produced from syncrude is expected to be higher than fossil-derived jet fuel. Therefore, the techno-economic analysis instead provides detailed process concepts with different technologies and a possible route to produce jet fuel from limited biomass resources. The technology described here could be employed to produce advanced biofuels and meet the requirement mandated by the Norwegian authority.

7 Conclusion

Six different BtL process concepts are compared and evaluated using process performance and economic analysis. The study consists of two conventional BtL concepts and four novel-BtL process concepts with SOEC integration. The process concepts were modeled in Aspen Plus flowsheeting simulation software, and economic analysis was performed utilizing available literature data and Aspen Capital Cost Estimator. The key conclusions of this study are listed below:

- The estimated minimum selling prices (MSPs) of syncrude are between $1.73~2.17/L for a BtL plant.
- All novel BtL process concepts with SOEC integration perform significantly better in maximizing total syncrude production and carbon efficiency.
- The energy efficiency of the conventional process can be improved by ca. 23% by operating FT synthesis at a lower H_2/CO ratio and higher overall CO conversion. These design principles also improve the carbon efficiency in the novel BtL process.
- With an electrical power price of $0.066/kWh and SOEC installation cost of $1,059/kW, the conventional BtL process with optimized fuel synthesis operation is the "Best Process Concept." The MSP of the syncrude for the best process concept is $1.73/L.
- The reverse water gas shift process has no added benefit in a novel BtL process with entrained flow gasification operating at high temperatures.
- Direct H_2 utilization and removing excess CO_2 have the best economic performance ("Best Process Concept") among the novel BtL concepts. The MSP for such a process is $1.79/L. Recycling excess CO_2 becomes more beneficial at cheaper electricity prices and SOEC costs.
- The process with direct H_2 utilization and recycling excess CO_2 would become the "Best Process Concept" at a reduced cost of SOEC. With a reduced SOEC installation cost of $230/kWh, the MSP of the syncrude for the process becomes $1.38/L.

Data availability statement

The original contributions presented in the study are included in the article/Supplementary Material, further inquiries can be directed to the corresponding author.

Author contributions

All authors listed have made a substantial, direct, and intellectual contribution to the work and approved it for publication.

Funding

The Research Council of Norway (project no. 280846) is greatly acknowledged for the financial aid of the project.

Conflict of interest

The authors declare that the research was conducted in the absence of any commercial or financial relationships that could be construed as a potential conflict of interest.

Publisher's note

Supplementary material

The Supplementary Material for this article can be found online at: https://www.frontiersin.org/articles/10.3389/fenrg.2022.993376/full#supplementary-material

References

Albrecht, F. G., König, D. H., Baucks, N., and Dietrich, R. U. (2017). A standardized methodology for the techno-economic evaluation of alternative fuels – a case study. *Fuel* 194, 511–526. doi:10.1016/j.fuel.2016.12.003

Banerjee, S. (2012). *Technoeconomic analysis of biorefinery based on multistep kinetics and integration of geothermal energy [Internet] [Master of Science]*. [Ames]: Iowa State University, Digital Repository, 4188199. Available from: https://lib.dr.iastate.edu/etd/12874/ (cited Feb 8, 2021).

Bernical, Q., Joulia, X., Noirot-Le Borgne, I., Floquet, P., Baurens, P., and Boissonnet, G. (2013). Sustainability assessment of an integrated high temperature steam electrolysis-enhanced biomass to liquid fuel process. *Ind. Eng. Chem. Res.* 52 (22), 7189–7195. doi:10.1021/ie302490y

Boie, W. (1953). Fuel technology calculations. *Energietechnik* 3, 309–316.

Carlsson, L. (2005). *From Bintulu Shell MDS to Pearl GTL in Qatar: Applying the lessons of eleven years of commercial GTL experience to develop a world-scale plant*. Malaysia: Shell MDS.

Dalai, A. K., and Davis, B. H. (2008). Fischer–tropsch synthesis: A review of water effects on the performances of unsupported and supported Co catalysts. *Appl. Catal. A General* 348 (1), 1–15. doi:10.1016/j.apcata.2008.06.021

Dieterich, V., Buttler, A., Hanel, A., Spliethoff, H., and Fendt, S. (2020). Power-to-liquid via synthesis of methanol, DME or fischer–tropsch-fuels: A review. *Energy Environ. Sci.* 13 (10), 3207–3252. doi:10.1039/d0ee01187h

Dietrich, R. U., Albrecht, F. G., Maier, S., König, D. H., Estelmann, S., Adelung, S., et al. (2018). Cost calculations for three different approaches of biofuel production using biomass, electricity, and CO2. *Biomass Bioenergy* 111, 165–173. doi:10.1016/j.biombioe.2017.07.006

Dimitriou, I., Goldingay, H., and Bridgwater, A. V. (2018). Techno-economic and uncertainty analysis of Biomass to Liquid (BTL) systems for transport fuel production. *Renew. Sustain. Energy Rev.* 88, 160–175. doi:10.1016/j.rser.2018.02.023

Dry, M. E. (2002). The fischer–tropsch process: 1950–2000. *Catal. Today* 71 (3), 227–241. doi:10.1016/s0920-5861(01)00453-9

Espinoza, R. L., Zhang, J., Wright, H. A., and Harkins, T. H. United States patent: Commercial fischer-tropsch reactor. US 7, 012, 103 B2, 2006. p. 11.

European Commission (2020). *Stepping up Europe's 2030 climate ambition: Investing in a climate-neutral future for the benefit of our people [Internet]*. Brussels: European Commission. Available from: https://eur-lex.europa.eu/legal-content/EN/TXT/PDF/?uri=CELEX:52020DC0562&from=EN (cited May 9, 2022).

Gavrilović, L., Brandin, J., Holmen, A., Venvik, H. J., Myrstad, R., and Blekkan, E. A. (2018). Fischer-tropsch synthesis—investigation of the deactivation of a Co catalyst by exposure to aerosol particles of potassium salt. *Appl. Catal. B Environ.* 230, 203–209. doi:10.1016/j.apcatb.2018.02.048

Haarlemmer, G., Boissonnet, G., Peduzzi, E., and Setier, P. A. (2014). Investment and production costs of synthetic fuels – a literature survey. *Energy* 66, 667–676. doi:10.1016/j.energy.2014.01.093

Hamelinck, C. N. (2004). *Outlook for advanced biofuels*. Utrecht: Universiteit Utrecht, Faculteit Scheikunde.

Hardeveld, R. M. V., Remans, T. J., and Stobbe, E. R. United States patent application publication: Stacked catalyst bed for fischer-tropsch. US 2013/0165537 A1, 2013.

Hillestad, M. (2015). Modeling the fischer–tropsch product distribution and model implementation. *Chem. Prod. Process Model.* 10 (3), 147–159. doi:10.1515/cppm-2014-0031

Hillestad, M., Ostadi, M., Alamo Serrano, G. d., Rytter, E., Austbø, B., Pharoah, J. G., et al. (2018). Improving carbon efficiency and profitability of the biomass to liquid process with hydrogen from renewable power. *Fuel* 234, 1431–1451. doi:10.1016/j.fuel.2018.08.004

Hofbauer, H., and Rauch, R. (2019). "Biomass to liquid (BtL)," in *Energy from organic materials (biomass): A volume in the encyclopedia of sustainability science and technology*. Editor M. Kaltschmitt. Second Edition (New York, NY: Springer), 1047–1063. (Encyclopedia of Sustainability Science and Technology Series).

Holmgren, K. M. (2015). *Investment cost estimates for gasification-based biofuel production systems*. Stockholm, Sweden: Swedish Environmental Research Institute.

Hoseinzade, L., and Adams, T. A. (2019). Techno-economic and environmental analyses of a novel, sustainable process for production of liquid fuels using helium heat transfer. *Appl. Energy* 236, 850–866. doi:10.1016/j.apenergy.2018.12.006

IEA. Global (2022). Energy review: CO2 emissions in 2021 [internet]. Available from: https://iea.blob.core.windows.net/assets/c3086240-732b-4f6a-89d7-db01be018f5e/GlobalEnergyReviewCO2Emissionsin2021.pdf (cited May 9, 2022).

James, R. E., Kearins, D., Turner, M., Woods, M., Kuehn, N., and Zoelle, A. (2019). *Cost and performance baseline for fossil energy plants volume 1: Bituminous coal and natural gas to electricity*. Pittsburgh: NETL.

Kargbo, H., Harris, J. S., and Phan, A. N. (2021). Drop-in" fuel production from biomass: Critical review on techno-economic feasibility and sustainability. *Renew. Sustain. Energy Rev.* 135, 110168. doi:10.1016/j.rser.2020.110168

Keçebaş, A., Kayfeci, M., and Bayat, M. (2019). "Chapter 9 - electrochemical hydrogen generation," in *Solar hydrogen production [internet]*. Editors F. Calise, M. D. D'Accadia, M. Santarelli, A. Lanzini, and D. Ferrero (Academic Press), 299–317.

Kolb, T., Eberhard, M., Dahmen, N., Leibold, H., Neuberger, M., Sauer, J., et al. (2013). *BtL - the bioliq® Process at KIT, preprints of the conference*. Germany, 7.

Kreutz, T. G., Larson, E. D., Elsido, C., Martelli, E., Greig, C., and Williams, R. H. (2020). Techno-economic prospects for producing Fischer-Tropsch jet fuel and electricity from lignite and woody biomass with CO2 capture for EOR. *Appl. Energy* 279, 115841. doi:10.1016/j.apenergy.2020.115841

Larson, E., Williams, R., Kreutz, T., Hannula, I., Lanzini, A., and Liu, G. Energy, environmental, and economic analyses of design concepts for the Co-production of fuels and chemicals with electricity via Co-gasification of coal and biomass. 2012. Report No.: 1047698.

Leibbrandt, N. H., Aboyade, A. O., Knoetze, J. H., and Görgens, J. F. (2013). Process efficiency of biofuel production via gasification and Fischer–Tropsch synthesis. *Fuel* 109, 484–492. doi:10.1016/j.fuel.2013.03.013

LOVDATA. Forskrift om begrensning i bruk av helse- og miljøfarlige kjemikalier og andre produkter (produktforskriften). § 3-5.Krav til oppfyllelse av bærekraftskriterier. 2022.

Michailos, S., and Bridgwater, A. (2019). A comparative techno-economic assessment of three bio-oil upgrading routes for aviation biofuel production. *Int. J. Energy Res.* 43 (13), 7206–7228. doi:10.1002/er.4745

Miljødirektoratet (2022). Biodrivstoff [internet]. Available from: https://www.miljodirektoratet.no/ansvarsomrader/klima/transport/biodrivstoff/(cited May 11, 2022).

Mýrdal, J. S. G., Hendriksen, P. V., Graves, C., Jensen, S. H., and Nielsen, E. R. (2016). *Predicting the price of solid oxide electrolysers (SOECs)*. Lyngby: Technical University of Denmark.

Neuling, U., and Kaltschmitt, M. (2018). Techno-economic and environmental analysis of aviation biofuels. *Fuel Process. Technol.* 171, 54–69. doi:10.1016/j.fuproc.2017.09.022

Norges Skogeierforbund (2018). Bruk av tre i produksjon av biodrivstoff [Internet]. Available from: https://skog.no/wp-content/uploads/2016/05/Bruk-av-tre-i-produksjon-av-biodrivstoff.pdf (cited May 22, 2022).

Pandey, U., Putta, K. R., Rout, K. R., Blekkan, E. A., Rytter, E., and Hillestad, M. (2022). *Staging and path optimization of Fischer-Tropsch synthesis*. Submitted to Chemical engineering research and Design.

Pandey, U., Runningen, A., Gavrilović, L., Jørgensen, E. A., Putta, K. R., Rout, K. R., et al. (2021). Modeling Fischer–Tropsch kinetics and product distribution over a cobalt catalyst. *AIChE J.* 67 (7), e17234. doi:10.1002/aic.17234

Putta, K. R., Pandey, U., Gavrilovic, L., Rout, K. R., Rytter, E., Blekkan, E. A., et al. (2022). Optimal renewable energy distribution between gasifier and electrolyzer for syngas generation in a power and biomass-to-liquid fuel process. *Front. Energy Res.* 9. [Internet]. doi:10.3389/fenrg.2021.758149

Qin, S., Chang, S., and Yao, Q. (2018). Modeling, thermodynamic and techno-economic analysis of coal-to-liquids process with different entrained flow coal gasifiers. *Appl. Energy* 229, 413–432. doi:10.1016/j.apenergy.2018.07.030

Rafati, M., Wang, L., Dayton, D. C., Schimmel, K., Kabadi, V., and Shahbazi, A. (2017). Techno-economic analysis of production of Fischer-Tropsch liquids via biomass gasification: The effects of Fischer-Tropsch catalysts and natural gas co-feeding. *Energy Convers. Manag.* 133, 153–166. doi:10.1016/j.enconman.2016.11.051

Ravaghi-Ardebili, Zohreh, Manenti, Flavio, Pirola, Carlo, Soares, Fiona, Corbetta, Michele, Pierucci, Sauro, et al. (2014). Influence of the effective parameters on h2:co ratio of syngas at low-temperature gasification. *Chem. Eng. Trans.* 37, 253–258.

Reed, M., and Bibber, L. V. (2007). *Baseline technical and economic assessment of a commercial scale fischer-tropsch liquids facility [internet]*. Morgantown: National Energy Technology Laboratory: DOE/NETL.

Rezaei, E., and Dzuryk, S. (2019). Techno-economic comparison of reverse water gas shift reaction to steam and dry methane reforming reactions for syngas production. *Chem. Eng. Res. Des.* 144, 354–369. doi:10.1016/j.cherd.2019.02.005

Sinnott, R., and Towler, G. (2019). *Chemical engineering design: SI edition*. Butterworth-Heinemann.

Spath, P. L., and Dayton, D. C. Preliminary screening – technical and economic assessment of synthesis gas to fuels and chemicals with emphasis on the potential for biomass-derived syngas. 2003;160. doi:10.2172/1216404

Storsæter, S., Borg, Ø., Blekkan, E. A., and Holmen, A. (2005). Study of the effect of water on Fischer–Tropsch synthesis over supported cobalt catalysts. *J. Catal.* 231 (2), 405–419. doi:10.1016/j.jcat.2005.01.036

Swanson, R. M., Platon, A., Satrio, J. A., and Brown, R. C. (2010). Techno-economic analysis of biomass-to-liquids production based on gasification. *Fuel* 89, S11–S19. doi:10.1016/j.fuel.2010.07.027

Swanson, R. M. (2009). *Techno-economic analysis of biomass-to-liquids production based on gasification [Graduate Theses and Dissertations]*. [Ames, Iowa]: Iowa State University.

Tijmensen, M. J. A., Faaij, A. P. C., Hamelinck, C. N., and van Hardeveld, M. R. M. (2002). Exploration of the possibilities for production of Fischer Tropsch liquids and power via biomass gasification. *Biomass Bioenergy* 23 (2), 129–152. doi:10.1016/s0961-9534(02)00037-5

Turton, R., Bailie, R. C., Whiting, W. B., and Shaeiwitz, J. A. (2008). *Analysis, synthesis, and design of chemical processes*. Prentice Hall, Upper Saddle River: Pearson Education.

Villanueva Perales, A. L., Reyes Valle, C., Ollero, P., and Gómez-Barea, A. (2011). Technoeconomic assessment of ethanol production via thermochemical conversion of biomass by entrained flow gasification. *Energy* 36 (7), 4097–4108. doi:10.1016/j.energy.2011.04.037

Zhu, Y., Tjokro Rahardjo, S. A., Valkenburt, C., Snowden-Swan, L. J., Jones, S. B., and Machinal, M. A. (2011). Techno-economic analysis for the thermochemical conversion of biomass to liquid fuels [internet]. Pacific northwest national lab. (PNNL), richland, WA (United States). Report No.: PNNL-19009. Available from: https://www.osti.gov/biblio/1128665/(cited Feb 2, 2021).

Nomenclature

Acronyms

ASF Anderson Schulz-Flory
ASU Air separation unit
BFW Boiler feed water
BtL Biomass to liquid
CAPEX Capital expenditure
CEPCI Chemical engineering plant cost index
CtL Coal to liquids
dtph dry tons per hour
FT Fischer-Tropsch
FTR Fischer-Tropsch reactors
GtL Gas to liquids
HHV Higher heating value
LHV Lower heating value
MSP Minimum selling price
OPEX Operating expenditure
RWGS Reverse water gas shift
SOEC Solid oxide electrolyzer cell
tph Tons per hour
WGS Water-gas shift
WHB Waste heat boiler
wtph Wet tons per hour

Greek symbols

α Chain growth parameter in FT polymerization reaction
η_B Boiler efficiency
η_C Carbon efficiency
η_e Energy efficiency
ν_i Stoichiometric coefficient of components i

Roman symbols

C_i Hydrocarbons with specified number of carbons
C_{24+} Hydrocarbons with 24 or more carbons
$C_{0,\text{Base year}}$ Equipment cost of the standard size in the base year (M$)
$C_{\text{direct},2022}$ Direct cost of specific equipment in 2022 (M$)
$C_{\text{direct,Base year}}$ Direct cost of specific equipment in the base year (M$)
$C_{\text{eq,Base year}}$ Equipment cost of the specific size in the base year (M$)
C_{inv} Total investment cost (M$)
dH_b Heating rate (MJ/tons of steam)
ΔG Gibbs free energy of formation of a compound (MW)
f_{building} Indirect cost factor for building
f_{com} Indirect cost factor for licenses and commissioning
f_{cont} Indirect cost factor for contingency
f_{dev} Indirect cost factor for project development
f_{eng} Indirect cost factor for engineering
f_{inst} Installation factor
f_{land} Indirect cost factor for land
f_{site} Indirect cost factor for site preparation
m_{Biomass} Mass flow of the biomass feed (kg/h)
m_{syncrude} Mass flow of the produced syncrude (kg/h)
MW_i Molecular weight of component i (kg/kgmole)
n Scaling factor
N_{np} Number of fluid processing units
N_{OL} Number of operators for fully automated process per shift
P Number of solid processing units
P_{BFW} Price of boiler feed water ($/tons of steam)
P_F Price of fuel ($/MJ)
P_{HPS} Price of HP steam ($/tons of steam)
Q Heat demand in the SOEC (MW)
S Specific size of the equipment
S_0 Standard size of the equipment
ΔS Change in entropy of the system (MW/K)
w_i Weight fraction component i
W Total electrical work in a BtL plant (MW)
W_E Electrical work in the SOEC (MW)